



Advanced 3-D electron kinetic calculations for the current drive problem in magnetically confined thermonuclear plasmas

Yves Peysson, J. Decker, A. Bers, B. Harvey, A. Ram

► To cite this version:

Yves Peysson, J. Decker, A. Bers, B. Harvey, A. Ram. Advanced 3-D electron kinetic calculations for the current drive problem in magnetically confined thermonuclear plasmas. 2004. hal-00002036

HAL Id: hal-00002036

<https://hal.science/hal-00002036>

Preprint submitted on 22 Oct 2004

HAL is a multi-disciplinary open access archive for the deposit and dissemination of scientific research documents, whether they are published or not. The documents may come from teaching and research institutions in France or abroad, or from public or private research centers.

L'archive ouverte pluridisciplinaire **HAL**, est destinée au dépôt et à la diffusion de documents scientifiques de niveau recherche, publiés ou non, émanant des établissements d'enseignement et de recherche français ou étrangers, des laboratoires publics ou privés.

Advanced 3 – D electron kinetic calculations for the current drive problem in magnetically confined thermonuclear plasmas

Y Peysson[†], J Decker[‡], A Bers[‡], R Harvey[§] and A Ram[‡]

[†] Association EURATOM-CEA sur la Fusion, CEA-Cadarache, F-13108 Saint Paul-lez-Durance, France

[‡] Plasma Science and Fusion Center, Massachusetts Institute of Technology, Cambridge, MA 02139, USA

[§]CompX, P.O. Box 2672, Del Mar, CA 92014-5672, USA

E-mail: yves.peysson@cea.fr

Abstract. Accurate and fast electron kinetic calculations is a challenging issue for realistic simulations of thermonuclear tokamak plasmas. Relativistic corrections and electron trajectory effects must be fully taken into account for high temperature burning plasmas, while codes should also consistently describe wave-particle resonant interactions in presence of locally large gradients close to internal transport barrier. In that case, neoclassical effects may come into play and self-consistent evaluation of both the radio-frequency and bootstrap currents must be performed. In addition, a complex interplay between momentum and radial electron dynamics may take place, in presence of a possible energy dependent radial transport. Besides the physics needs, there are considerable numerical issues to solve, in order to reduce computer time consumption and memory requirements at an acceptable level, so that kinetic calculations may be valuably incorporated in a chain of codes which determines plasma equilibrium and wave propagation. So far, fully implicit 3-D calculations based a finite difference scheme and a incomplete LU factorization have been found to be so most effective method to reach this goal. A review of the present status in this active field of physics is presented, with an emphasis on possible future improvements.

PACS numbers: 52.55.Fa, 52.65.Ff, 52.55.Wq

1. Current drive modeling issues

Since it has been recognized ten years ago that current drive efficiencies of available methods were far too low for sustaining all the toroidal current in a burning plasma with a reduced fraction of the alpha power, the picture of a steady-state tokamak reactor has deeply changed [1]. This led to the emergence of the well known advanced tokamak concept [2], where the plasma self-generates most of its current from steep pressure gradient, whose profile should be, in principle, naturally consistent with the magnetic equilibrium. In this regime, one takes benefit of neoclassical effects at high β_p , where the bootstrap current resulting from radial drift predominates. External current sources are therefore viewed as a complement for full steady-state operation, and tools for a local control of the current density profile which plays a central role in plasma performances and stability.

Consequently, modeling issues for current drive has considerably evolved since the pioneering studies, which were principally focused on the problem of efficiency for reducing the recycling power [3]. Indeed, since advanced scenarios are designed primarily for reducing the need of external sources of current, the question of the efficiency became progressively marginal, though several attempts to improve performances by potential synergistic effects have been performed both from the theoretical and experimental point of view [4]. So far, no breakthrough in this domain has been achieved, and most of the conclusions drawn in the early 90's remain still valid.

Conversely, the need for an accurate current localization in very narrow region of the plasma where pressure gradients may be steep has considerably increased, mainly for a precise control of transport barrier whose presence is expected to be strongly beneficial for fusion plasma performances (H-mode edge pedestal, internal transport barrier). Stabilizing neoclassical tearing modes by very local current drive for avoiding degradation of the plasma confinement is also an important issue [5]. The goal of an accurate current drive localization represents an important challenge for both physics and technology, regarding the fact that current density profile must be tuned easily from a few set of external parameters of the heating system, in view to achieve real time control in fully non inductive operation. For the RF current drive, the usual approach is to split the problem into two parts, one concerning the electromagnetic propagation of the wave in the plasma and the other being dedicated to the kinetic wave-particle interaction describing momentum transfer and the related absorption process. In both cases, credible simulations on which most of the complex fusion scenarios are based, require to describe physics problem in a very realistic way. Moreover, these simulations often represent a major challenge from the numerical point of view, since both magnetic equilibrium and transport properties must be self-consistently determined with wave propagation and absorption. Therefore, kinetic calculations for the current drive problem, as part of a chain of codes must provide a quick and precise manner the correct answer regarding the physics processes that are described. Here, only kinetic calculations concerning the electron population are addressed.

1.1. Physics requirements

In the low collision limit that prevails in the core region of a hot tokamak plasma, which is characterized by the well know parameter $\nu^* \equiv \tau_b/\tau_{dt} \ll 1$, where τ_b and τ_{dt} are respectively the bounce and collisional detrapping times for trapped particles, the current drive problem is basically a 3 – D kinetic problem, 2 – D in momentum space characterized by the impulsion p and pitch-angle cosine ξ_0 coordinates[‡], and 1 – D in configuration space, where the coordinate ψ chosen for labeling concentric magnetic flux surfaces is the poloidal magnetic flux. Both circulating and trapped electrons may therefore complete their trajectories in a poloidal plane section, before being scattered-off from their trajectory by collisions, so that the bounce-averaged Fokker-Planck equation must be the starting point of all kinetic calculations for realistic current drive simulations. For electrons, in the small drift approximation, the banana width is always very small regarding the gradient length scales, and bounce-averaging provides the correct method §.

The detailed aspects of the magnetic equilibrium are also very important, in particular when physics must be described close to the plasma edge, where interplay between trapped and circulating electrons may have an important role. In region of the plasma where pressure gradient is large, neoclassical corrections must be described, leading to solve the electron drift kinetic equation by a perturbative technique, instead of the usual Fokker-Planck equation [6]. In that regime, the lack of symmetry of the distribution function in momentum space which leads to the bootstrap current, may modify the wave-particle interaction, leading to potential synergistic effects.

Additional physical ingredients must be added for realistic simulations. Fully relativistic description must be carried out, in order to describe hot plasma physics ($T_e > 2 - 3keV$) and also the dynamics of very energetic electron tail that can be produced by RF waves. Moreover, the difficult question of fast electron radial transport must be also addressed [7], since it may completely change the ability to control the local current density. Not only the usual possible contribution of plasma turbulence must be considered, but also radial transport that could result itself from wave momentum transfer to the electron population. Indeed, in toroidal device, the conservation of the generalized toroidal momentum in axisymmetric configuration implies that a strong variation of the velocity corresponds to a radial jump, leading to a potential broadening of the driven current. Cross-diffusion terms between momentum and configurations spaces may play therefore an important role.

[‡] The pitch-angle is taken with respect to the magnetic field line direction, which is considered to be an axis of symmetry.

§ For ion physics, orbit averaging is fully needed, since orbits are large as compared to all gradient lengths in the plasma

1.2. Numerical requirements

Since the collision time is usually much lower than characteristic energy or resistive current diffusion times, self-consistent current drive calculations require the determination of the steady-state solution. Therefore, numerical algorithms should provide fast rate of convergence towards this asymptotic value, which implies implicit or reverse time differencing [8]. However, very large integration time step Δt may be used without onset on numerical instabilities only when the full 3 – D dynamics is considered as a whole^{||}. Operator splitting between momentum and configuration dynamics, that is currently used in existing 3 – D Fokker-Planck calculations leads always to strong limitations on Δt , which thus hinder the advantage to perform implicit calculations in each subspace. So far, full 3 – D implicit method required advanced computing techniques, owing to the very large size of the matrix that must be inverted. The conservative nature of the Fokker-Planck solver for the particles and momentum is also a crucial point for the reliability of the results, but also for ensuring a fast rate of convergence. Finally, it is well known that matrix conditioning is an important criterion for fast calculations [9]. This difficult problem must be clearly addressed, by considering limitations that result both from the physics assumptions of the model, and the discrete form of the equations.

2. Tokamak Fokker-Planck code status

Fokker-Planck calculations are widely used in tokamak plasma physics, and so far have proven their effectiveness for describing intimate aspects of the particle dynamics at the microscopic scale. The Electron Cyclotron current drive studies is a very good example for this purpose [10].

Numerous solvers have been dedicated for the current drive problem since the last 25 years. They represent an heterogenous family of 20 codes approximately, mostly developed for solving specific physics problem by independent groups. They are principally stand-alone applications which are often characterized by poor documentation and reduced maintenance. This makes the situation quite puzzling, while the need for realistic simulations in reactor like conditions has considerably increased over the years. Surprisingly, while the objectives for current drive applications have drastically changed since the beginning of the 90's, most of the dedicated tools which are still in use today have been developed far before this period, in the 80's, and often for completely different purposes. Except the *CQL3D* code [11], it is therefore not surprisingly that most of them are not designed for high β_p regime though describing the 3 – D dynamics, using oversimplified magnetic equilibrium with circular and concentric flux surfaces [12, 13]. So far, only one simulation package CRONOS uses bounce-averaged relativistic 3 – D Fokker-Planck solvers for Lower Hybrid current drive calculations [9, 14], while several others, [15, 16], have still a 1 – D non-relativistic

^{||} Here Δt is normalized to the collision time

Fokker-Planck code for Lower Hybrid power absorption for example [17].

The bootstrap current is never evaluated self-consistently with RF current sources in high β_p regime, and attempts for solving the drift kinetic equation for non-Maxwellian distribution (electron and ion) and arbitrary magnetic equilibrium have not given so far convincing results nor the emergence of a production code [18]. In *CQL3D*, the bootstrap current is evaluated from kinetic calculations but using a quite crude technique by adding an effective particle source at the trapped-passing boundary [19]. If such an approach is acceptable for a Maxwellian regime, as confirmed by the reasonable agreement between code results and theoretical expectations within 20%, this method is questionable for non-Maxwellian regime. Recent interesting developments have been made for electrons, but using a simplified equilibrium at low β_p , leading nevertheless to promising results concerning potential synergistic effects [6].

The Fokker-Planck codes that address the 2 – D or 3 – D kinetic problem may be divided roughly in two groups: slow solvers mainly based on Monte-Carlo technique, and faster tools based on finite difference technique. Other numerical methods may be found in the literature for solving the 2 – D Fokker-Planck equation, but they represent marginal though interesting developments. Most codes designed for the current drive problem are based on finite differencing. While Monte-Carlo codes usually allows a detailed and realistic description of the particle dynamics, in particular toroidal effects for wave-particle interactions [20], fast solvers based on finite differencing uses simplified quasilinear diffusion operators for plane waves that prevents studies of cross-effects between momentum and configuration spaces [21, 22].

From the numerical point of view, existing solvers based on finite differencing use operator splitting technique [8], which strongly reduces the rate of convergence towards the steady-state solution, with $\Delta t \lesssim 1$. It is interesting to mention the pioneering work to demonstrate the feasibility of fast fully implicit 3 – D steady-state Fokker-Planck calculations, with the *RFTRANS* code [23]. Though designed for ion RF heating, and simplified configuration with no particle trapping, it has been possible to determine the solution in 6 iterations on a CRAY-2, with a $128 \times 32 \times 11$ mesh. However, at that time computer capabilities were quite limited, and each iteration took 1 – 2 hour. Along the same spirit, partial *LU* matrix factorization has been shown to be a very effective method for fully implicit calculations involving very large matrices for 2 – D or 3 – D Fokker-Planck current drive calculations. In that case again, no trapping was considered [9].

From this brief review, it is clear that kinetic calculations for current drive in hot thermonuclear plasmas require new tools, which both incorporate advanced physics concepts, but also optimized numerical methods. The development of a fast drift kinetic solver for the electron population is a logical consequence of the needs that emerge today in advanced tokamak scenario for an accurate control of the fusion performances.

3. Fast 3-D drift kinetic solver for electrons

3.1. Basic equations

The starting point of the calculations is the gyro- and wave-averaged guiding center Fokker-Planck equation. Here arbitrary axisymmetric tokamak magnetic configuration is considered, the magnetic flux surfaces being labeled by the poloidal flux coordinate ψ . In the small drift approximation $\delta \equiv \tau_b/\tau_{drift} \ll 1$, where τ_{drift} is the vertical drift time, the distribution function f may be expanded as $f = f_0 + f_1$, f_1 being of the order of δ . The zero order equation referred usually to as the Fokker-Planck equation is

$$v_s \frac{\partial f_0}{\partial s} = \mathcal{C}(f_0) + \mathcal{Q}(f_0) + \mathcal{E}(f_0) \quad (1)$$

while the first order equation

$$v_s \frac{\partial f_1}{\partial s} + \frac{v_{\parallel}}{\Omega_e} I(\psi) \frac{|\nabla \psi|}{R} \frac{\partial}{\partial s} \left(\frac{v_{\parallel}}{B} \right) \frac{\partial f_0}{\partial \psi} = \mathcal{C}(f_1) + \mathcal{Q}(f_1) + \mathcal{E}(f_1) \quad (2)$$

is referred to as the electron drift kinetic equation. Here v_{\parallel} is the parallel component of the velocity with respect to the local magnetic field direction $\hat{B}/|B|$, where $B = RI(\psi)$, R being the major radius, Ω_e the cyclotron frequency, s and v_s the curvilinear coordinate and velocity along the magnetic field line. The operators \mathcal{C} , \mathcal{Q} and \mathcal{E} refer to collisions, RF quasilinear diffusion and Ohmic electric field acceleration respectively. The fully relativistic Belaiev-Budker collision operator with up to first order Legendre correction for momentum conservation is used in the calculations [24, 25]

In the small banana width approximation, and for the banana regime $\nu^* \ll 1$, both equations may be bounce-averaged, the annihilator of the poloidal dependence taking the general form

$$\{\mathcal{A}\} = \frac{1}{\lambda \tilde{q}} \left[\frac{1}{2} \sum_{\sigma} \right]_T \int_{\theta_{\min}}^{\theta_{\max}} \frac{d\theta}{2\pi} \frac{1}{|\hat{\psi} \cdot \hat{r}|} \frac{r}{R_p} \frac{B}{B_P} \frac{\xi_0}{\xi} \mathcal{A} \quad (3)$$

where θ is the poloidal angle, λ the bounce time normalized to the transit time, R_p the major radius of the plasma center, B_P the poloidal magnetic field, $\sigma = \xi_0/|\xi_0|$ and $[\frac{1}{2} \sum_{\sigma}]_T$ indicates that the sum only concerns trapped electrons. Here, $r = \sqrt{(R - R_p)^2 + (Z - Z_p)^2}$ where Z is the vertical position on the flux surface at the poloidal angle θ , Z_p the vertical position of the plasma center and the scalar product $\hat{\psi} \cdot \hat{r}$ takes into account of the plasma shape while $\tilde{q}(\psi) = \int_0^{2\pi} \frac{d\theta}{2\pi} \frac{1}{|\hat{\psi} \cdot \hat{r}|} \frac{r}{R_p} \frac{B}{B_P}$. The pitch-angle cosine ξ at taken poloidal angle θ , and its value where the magnetic field is minimum is ξ_0 . In this regime, f_0 is constant on a flux surface, since $\{v_s \frac{\partial f_0}{\partial s}\} = 0$, and f_0 is determined by the well know bounce averaged equation

$$\{\mathcal{C}(f_0)\} + \{\mathcal{Q}(f_0)\} + \{\mathcal{E}(f_0)\} = 0. \quad (4)$$

Using similar arguments, the left handside of Eq. 2 may be easily integrated as function of s , and using $f_1 = \tilde{f} + g$, it can shown that $\tilde{f} = \frac{v_{\parallel}}{\Omega_e} I(\psi) \frac{\partial f_0}{\partial \psi}$, and the bounce

averaged drift kinetic equation is $\{\mathcal{C}(f_1)\} + \{\mathcal{Q}(f_1)\} + \{\mathcal{E}(f_1)\} = 0$. Since all operators are linear, the function g is determined by the equation

$$\{\mathcal{C}(g)\} + \{\mathcal{Q}(g)\} + \{\mathcal{E}(g)\} = -\left\{\mathcal{C}(\tilde{f})\right\} - \left\{\mathcal{Q}(\tilde{f})\right\} - \left\{\mathcal{E}(\tilde{f})\right\} \quad (5)$$

It is important to note that \tilde{f} is an antisymmetric function of ξ , while g is symmetric. Therefore bounce-averaged operator for f_0 and g are similar, while values are different for \tilde{f} .

Nevertheless, it can be shown that both Eqs. 4 and 5 may be cast in a conservative form. For the zero order term $\frac{\partial f_0^{(0)}}{\partial t} + \nabla_{(\psi,p,\xi_0)} \cdot \mathbf{S}^{(0)} = 0$, where superscript (0) indicates that quantity is taken where B is minimum. Here $\mathbf{S}^{(0)}(f_0^{(0)}) = -\mathbb{D}^{(0)} \nabla_{(\psi,p,\xi_0)} f_0^{(0)} + \mathbf{F}^{(0)} f_0^{(0)}$ is the generalized flux function in 3 – D space, where $\mathbb{D}^{(0)}$ is the diffusion tensor and $\mathbf{F}^{(0)}$ the convection vector. The divergence term, which may be deduced from first principle particle, energy and magnetic moment conservations, is given by

$$\begin{aligned} \nabla_{(\psi,p,\xi_0)} \cdot \mathbf{S}^{(0)}(f_0^{(0)}) &= \frac{1}{p^2} \frac{\partial}{\partial p} (p^2 \mathbf{S}_p^{(0)}) - \frac{1}{\lambda} \frac{1}{p} \frac{\partial}{\partial \xi_0} \left(\sqrt{1 - \xi_0^2} \lambda \mathbf{S}_\xi^{(0)} \right) \\ &\quad + \frac{B_0}{\lambda \tilde{q}} \frac{\partial}{\partial \psi} \left(\frac{\tilde{q}}{B_0} \lambda |\nabla \psi|_0 \mathbf{S}_\psi^{(0)} \right) \end{aligned} \quad (6)$$

where the first two terms of the left handside correspond to momentum slowing-down at pitch-angle scattering respectively, and the third one to the radial dynamics. It is worth noting that radial and pitch-angle dynamics are strongly link because of magnetic moment conservation. Here B_0 is the total magnetic field taken at the poloidal position where it is minimum, and $\mathbf{S}_p^{(0)}$, $\mathbf{S}_\xi^{(0)}$ and $\mathbf{S}_\psi^{(0)}$ are the three components of $\mathbf{S}^{(0)}$ in the space here considered[¶]. A similar expression may be obtained for g and \tilde{f} but only in momentum space in that case, where $\mathbf{S}_p^{(0)}(g^{(0)}) = \mathbf{S}_p^{(0)}(f_0^{(0)})$ and $\tilde{\mathbf{S}}_p^{(0)}(\tilde{f}^{(0)}) = -\tilde{\mathbb{D}}_p^{(0)} \nabla_{(p,\xi_0)} \tilde{f}^{(0)} + \tilde{\mathbf{F}}_p^{(0)} \tilde{f}^{(0)}$. This result has important consequences: first, a unified formalism may be used for solving both Eqs. 4 and 5, so that the same numerical conservative scheme may be applied. Furthermore, a simple picture emerges for the Maxwellian bootstrap current which just results from the fact that $\tilde{F}_\xi^{(0)} = \left\{ \frac{\xi^2}{\Psi^{3/2} \xi_0^2} F_\xi \right\} + \frac{\sqrt{1 - \xi_0^2}}{p \xi_0^3} \sigma \left\{ \frac{\sigma \xi (\Psi - 1)}{\xi_0 \Psi^2} D_{\xi\xi} \right\} \neq 0$, leading to a deformation of $f^{(0)}$ in momentum space, when the first order term is considered. Here $\Psi = B/B_0$.

3.2. Numerical solver

The numerical solver is based on a standard finite implicit difference technique, using two non-uniform interlaced grids for each coordinate p, ξ_0 and ψ , one for the fluxes, the other for the distribution itself. Linear interpolation is performed between flux and distribution grids for ξ_0 and ψ , while a specific development is performed for p so that numerical errors are exponentially small, a primary condition for recovering the Maxwellian solution when only collisions are at play [26]. Bounce integrals are performed

[¶] It is convenient to define $\mathbf{S}_p^{(0)}$ as the flux in momentum subspace only

numerically from a magnetic equilibrium solver [27], taking special care for banana tips contribution. Spatial gradients for determining $\partial f_0/\partial\psi$ are calculated using a 3-points parabolic interpolation, so that self-consistent calculations involving bootstrap current require a radial mesh size that is 3 times larger than for usual Fokker-Planck calculations. The shape of the matrix for the Fokker-Planck equation is given in Fig. 1. It is made of blocks of 15 diagonals describing the momentum dynamics, whose size decreases as ψ rises, because the trapped/passing boundary depends of the radial position. Each block is connected with its neighboring one by several diagonals concerning radial transport, which may cause particle trapping or detrapping. The matrix for the function g is less complex though its shape is similar, since each block describing momentum dynamics has only 9 diagonals, without diagonal link between blocks as shown in Fig. 2.

As the number of grid points may reach $n_p \simeq 200$, $n_\xi \simeq 200$ and $n_\psi \simeq 20 - 40$ for accurate current drive calculations, the dimension of the matrices are very large, leading to a challenging problem for the inversion procedure. Furthermore, since several iterations are required because of non-linear corrections resulting from the collision term momentum conservation, an iterative procedure is considered. In that case, the LU matrix factorization is the most useful method, since the computational effort for the factorization procedure is comparable to a single inversion. Once done, other inversions are much faster [8]. However, in order to reduce the huge non-zero coefficients of matrices L and U , a partial factorization technique instead of an exact one is employed, based on a coefficients pruning [28]. Under a drop tolerance criterion δ_{lu} , coefficients are forced to zero. From $\delta_{lu} = 0$ to $\delta_{lu} = 10^{-3}$, a gain of 30 may be obtained on the reduction of the memory storage requirement while convergence is achieved on a shorter duration, without changing the solution, as shown in Fig. 3. This method has proven to be well adapted to the Fokker-Planck problem, since it is basically well conditioned. The main diagonal matrix is dominant, since coefficients corresponding to collision pitch-angle scattering exceed those of slowing-down and radial transport. When this ordering is only slightly perturbed by an Ohmic electric field or RF quasilinear diffusion, the numerical stability remains excellent. When very large coefficients off the main diagonal appear, the matrix conditioning becomes poor, leading usually to unphysical solutions. However, a detailed insight shows that these cases correspond mostly to physical situations that are not compatible with the assumptions used for deriving the model.

In Figs. 4, 6, 5, 7, 8 and Figs. 9, 10, two examples of code performances are shown. All calculations are performed with $\Delta t = 10000$ and $\delta_{lu} = 10^{-4}$. For Lower Hybrid current drive in JET tokamak equilibrium in presence of a radial transport that scales with $v_{||}$ above $v/v_{th} = 3.5$, where v_{th} is the thermal velocity taken in the center of the plasma, a grid $n_p n_\xi n_\psi \simeq 200 \times 200 \times 14$ is considered. The solution at all radii is found in 20 minutes CPU on a standard UNIX workstation. A minimum of 6 iterations is enforced for an accurate current determination. The Maxwellian bootstrap current for Tore Supra requires 42 spatial points because of gradients calculations. Here $n_p n_\xi n_\psi \simeq 200 \times 100 \times 42$, and the solution at the 14 effective grid points is obtained in 5 minutes on the same computer. A very good agreement is found with Hirshman and

Sauter relations at all radii [29, 30]. When the well known L_{32} neoclassical coefficient differs, it is found that code prediction are in better agreement with Sauter relation [30]. The lack of agreement with Hinton relation arises from the fact that the effective charge of the plasma exceeds unity in the simulation [31]. For all simulations, the ion bootstrap current contribution in the code is deduced from Hirshman law, determined in the fluid limits [29]. Excellent agreement with the Lorentz gas model is found not only for the moments of the distribution, but also for the distributions $\tilde{f}^{(0)}$ and $g^{(0)}$.

Concerning potential synergies between bootstrap current and RF current, results obtained at low β_p are confirmed [6], in particular the fact that the scaling is proportional to the target Maxwellian bootstrap current. Indeed, the bootstrap current results in an accumulation of circulating electrons close to the trapped/passing boundary in the positive momentum direction with respect to the sign conventions here used, and this excess of particle may be very beneficial to pull out a tail from the bulk. Results for large β_p have not yet being fully investigated so far, but promising results are expected with this new code for reactor relevant conditions.

Finally, the kinetic code allows calculation of numerous interesting macroscopic moments of the distribution function, in addition to the current itself: the power absorbed by collisions, the RF and Ohmic powers, the runaway and magnetic ripple loss rate, the non-thermal bremsstrahlung, the effective and exact trapped fractions, all of them given an insight of the physical processes at play.

Further important developments are foreseen in a very near future. The most important step is to perform orbit averaging instead of bounce-averaging. This approach will give access to the ion physics including anomalous potato orbits [32]. Therefore, a fast multispecies Fokker-Planck code may be designed, taking benefit from the existing non-uniform momentum grid at low energy for the ion dynamics. From the general Hamiltonian formalism in toroidal device that is needed, it is also possible to derive a RF quasilinear diffusion coefficient for the electrons that naturally incorporates cross-effects between momentum and radial spaces [20]. Study of the influence of the wave induced radial transport on RF power deposition will be then possible.

References

- [1] Rebut P H, 1993 *Plasma Phys. Control. Fusion* **35** A1
- [2] Taylor T, 1997 *Plasma Phys. Control. Fusion* **39** B47
- [3] Karney C F F and Fisch N J, 1985 *Phys. Fluids* **B28** 116
- [4] Peysson Y, 1999 *13th Conference on Radio Frequency Power in Plasma, Annapolis, USA* (AIP Conference Proceedings) Vol 485 p 183
- [5] Giruzzi G et al., 1999 *13th Conference on Radio Frequency Power in Plasma, Annapolis, USA* (AIP Conference Proceedings) Vol 485 p 35
- [6] Schultz S, 1999 *Lower Hybrid and Electron Cyclotron Current Drive With Bootstrap Current in Tokamaks*(MIT thesis, Cambridge, USA)
- [7] Peysson Y, 1993 *Plasma Phys. Control. Fusion* **35** B253
- [8] Press W H et al., 1992 *Numerical Recipes in C, 2th Edition* (Cambridge University Press)
- [9] Peysson Y and Schoucri M, 1998 *Comp. Phys. Comm.***109** 55

- [10] Prater R, 2004 *Phys. Plasma* **11** 2349
- [11] Harvey R W and McCoy M G, 1993 *IAEA Technical Committee on Advances in Simulation and Modeling of Thermonuclear Plasmas* 489
- [12] McKenzie J S et al., 1986 *Nucl. Fusion* **26** 12
- [13] Giruzzi G, 1988 *Phys. Fluids* **28** 3305
- [14] Basiuk V et al., 2003 *Nucl. Fusion* **43** 822
- [15] Genacchi G and Taroni A, 1988 *Report ENEA RT/TIB* 5
- [16] Pereverzev G and Yushmanov P N, 2002 *Report IPP* 5/98
- [17] Esterkin A R and Piliya A D, 1996 *Nucl. Fusion* **36** 1501
- [18] Zaitsev F S et al., 1993 *Phys. Fluids B* **5** 509
- [19] Westerhof E and Peeters A G, 1996 *Comp. Phys. Comm.* **95** 131
- [20] Eriksson L -G and Helander P, 1994 *Phys. Plasmas* **1** 308
- [21] Kennel C F and Engelmann F, 1966 *Phys. Fluids* **9** 2377
- [22] Lerche I, 1968 *Phys. Fluids* **11** 1720
- [23] Carter M D et al., 1989 *Nucl. Fusion* **29** 2141
- [24] Braams B J and Karney C F F, 1989 *Phys. Fluids B* **1** 1355
- [25] Shkarofsky I P and Shoucri M M, 1997 *Nucl. Fusion* **37** 539
- [26] Bizarro J P S and Rodrigues P, 1997 *Nucl. Fusion* **37** 1509
- [27] Huysmans G T A et al., 1991 *Proc. CP90 Conf. Comp. Physics* (Singapore:Word Scientific) p 371
- [28] Saad Y, 2003 *Iterative Methods for Sparse Linear Systems, 2nd Edition* (Society for Industrial and Applied Mathematics)
- [29] Hirshman S P, 1988 *Phys. Fluids B* **31** 3150
- [30] Sauter O et al., 1999 *Phys. Plasma* **6** 2834
- [31] Hinton F L and Hazeltine R D, 1976 *Rev. of Mod. Physics* **48** 239
- [32] Eriksson L -G and Porcelli F, 2002 *Nucl. Fusion* **42** 959

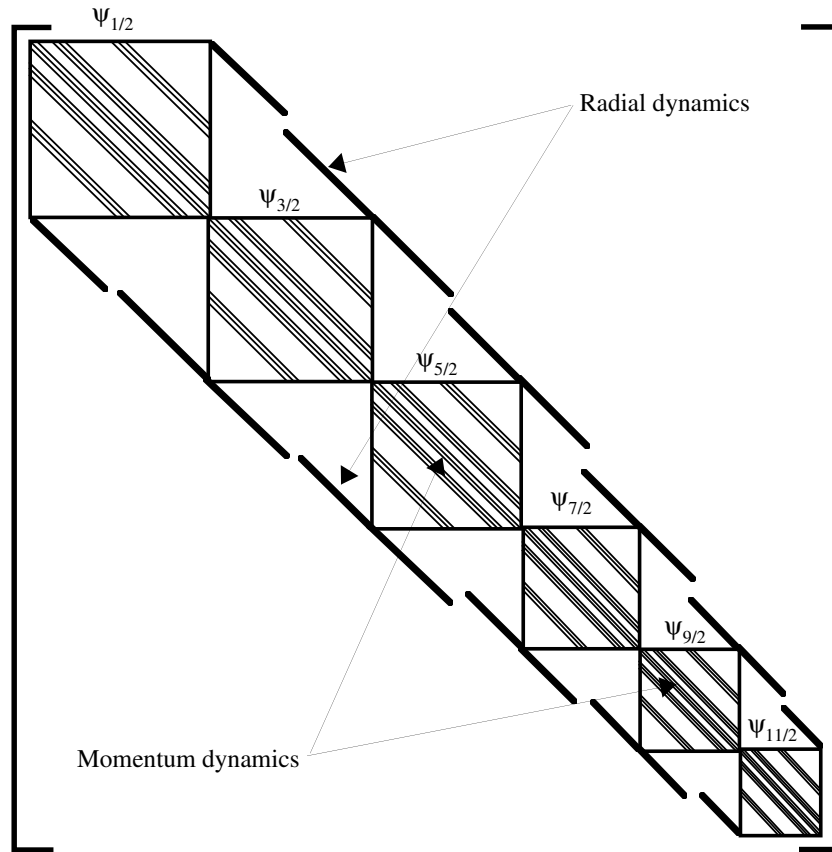


Figure 1. Qualitative shape of matrix used for solving the zero order Fokker-Planck equation.

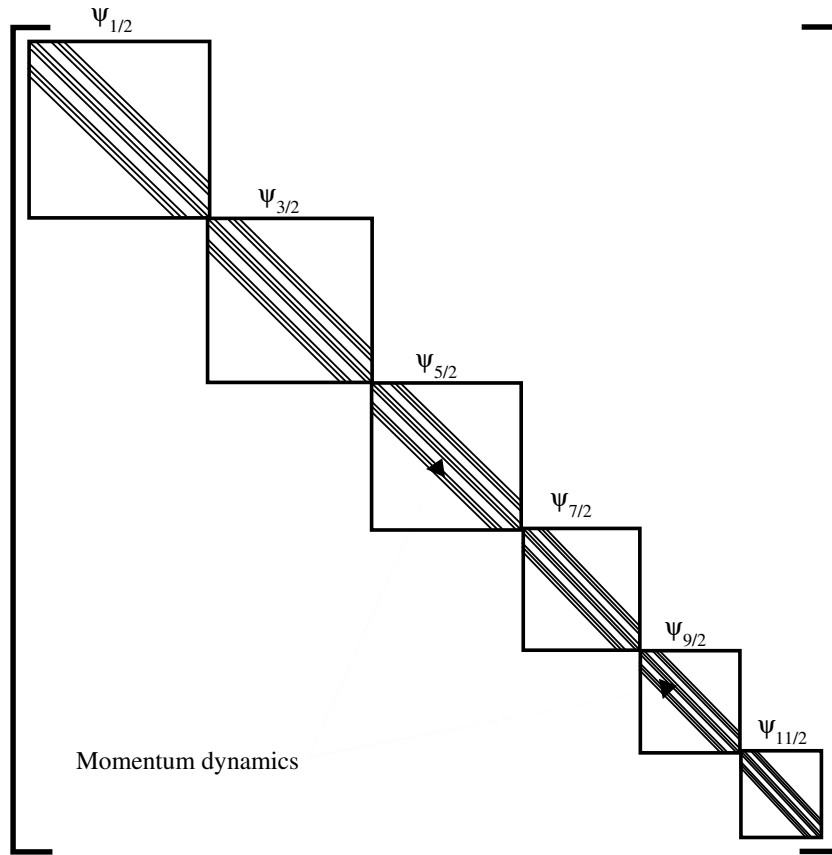


Figure 2. Qualitative shape of matrix used for solving the first order drift kinetic equation.

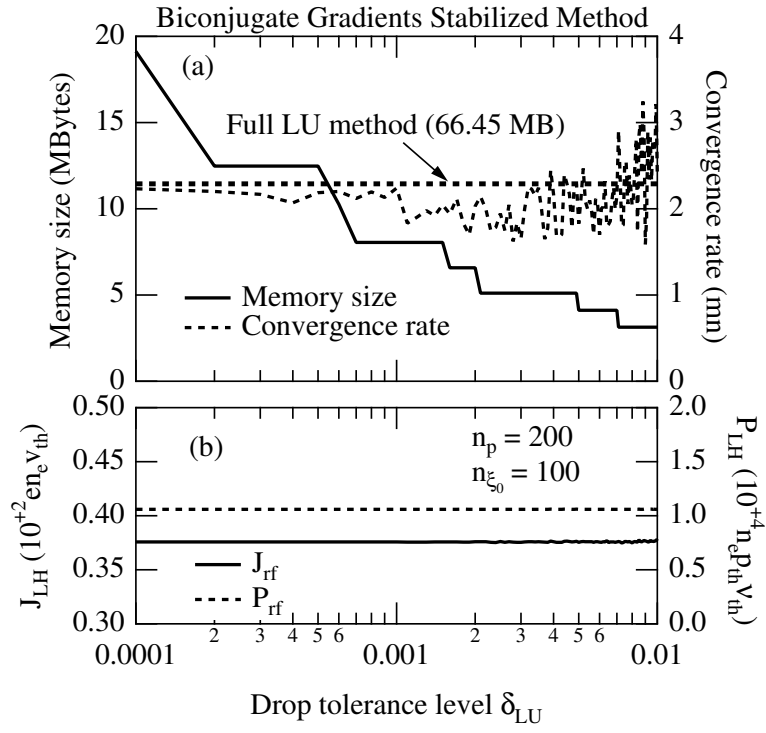


Figure 3. Memory storage requirement reduction by increasing the δ_{lu} parameter, for the Lower Hybrid current drive problem. The rate of convergence towards the steady state solution is given, using the biconjugate gradient stabilized method to solve the system of linear equations. Here only a local analysis is considered at a given radial position

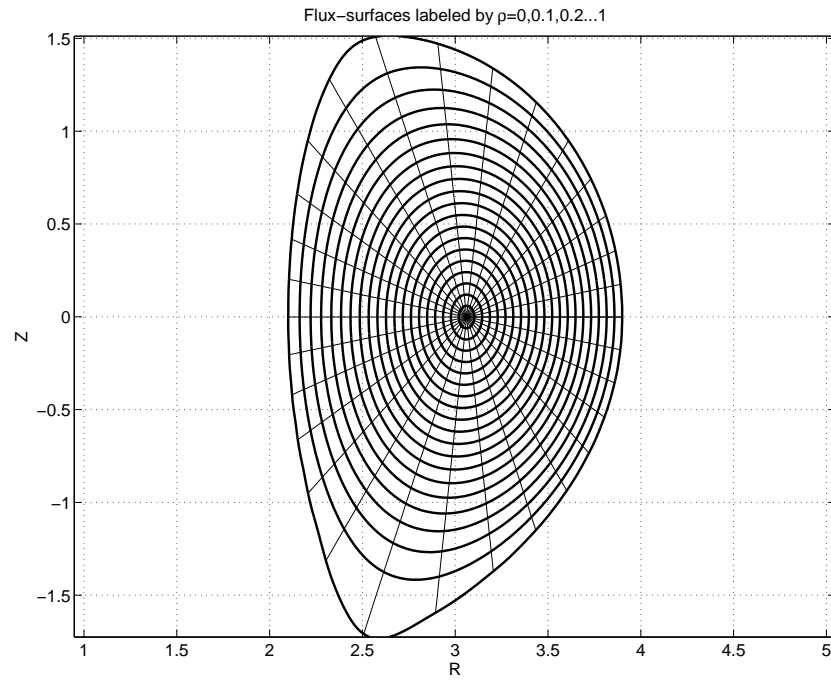


Figure 4. 2 – D contour plot of the poloidal magnetic flux surfaces as calculated for JET tokamak by the code HELENA.

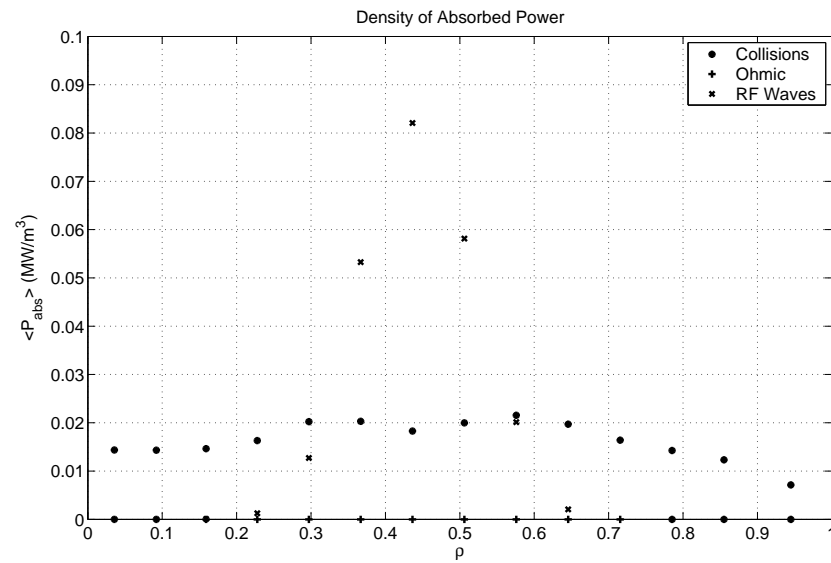


Figure 5. Flux surface averaged power density profiles for collision, RF and Ohmic electric field absorption for the 3 – D JET Lower Hybrid current drive simulation.

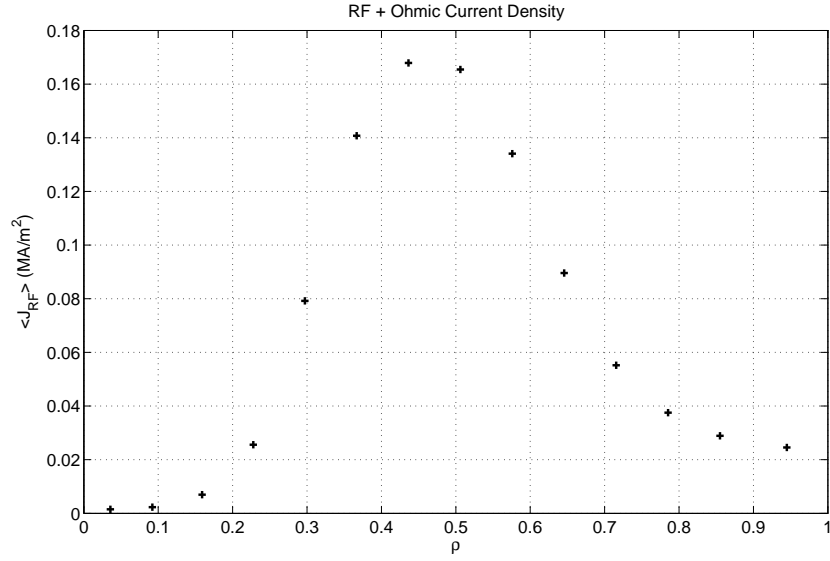


Figure 6. Flux surface averaged current density profiles for the 3 – D JET Lower Hybrid current drive simulation.

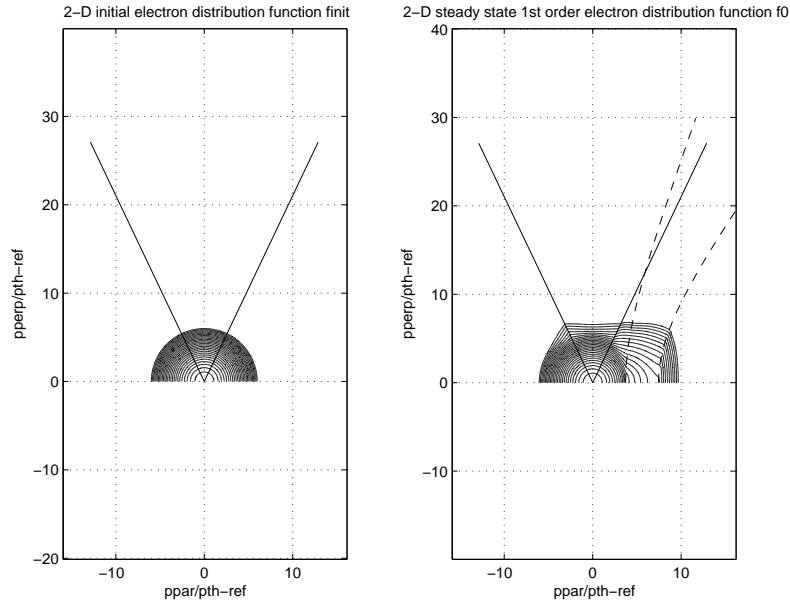


Figure 7. 2 – D contour plot of the electron distribution function at $\rho \simeq 0.36$ for JET before and after onset of Lower Hybrid current drive. Here the non-thermal electrons result principally from quasilinear acceleration though fast electron radial transport is at play

f2DpeakJET7cm

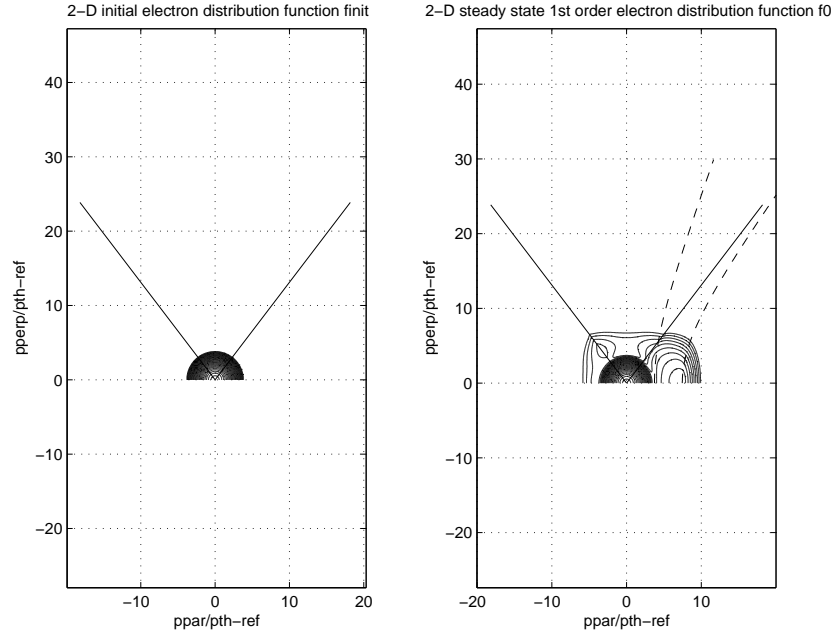


Figure 8. 2 – D contour plot of the electron distribution function at $\rho \simeq 0.78$ for JET before and after onset of Lower Hybrid current drive. Here the non-thermal electrons result only from anomalous radial transport

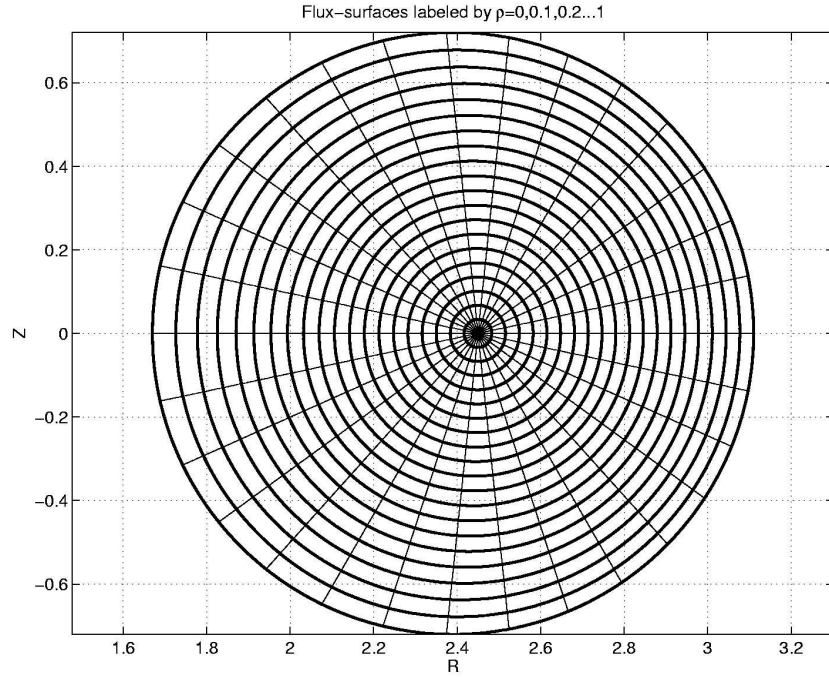


Figure 9. 2 – D contour plot of the poloidal magnetic flux surfaces as calculated for Tore Supra tokamak by the code HELENA.

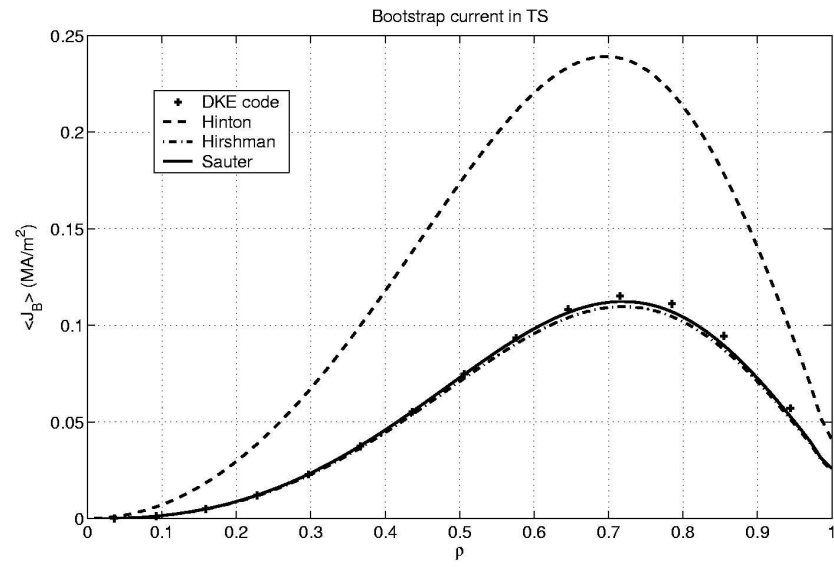


Figure 10. Bootstrap current profile given by the drift kinetic code for the Tore Supra magnetic configuration and different corresponding analytical formulas (see the text for more details).